Improvement of Transient Stability in the Galápagos Hybrid System using and UPFC

Carlos Gallardo

Faculty of Electrical and Electronic Engineering, Escuela Politécnica Nacional, Quito, Ecuador.

Mayra Espinoza

Faculty of Chemical Sciences, Escuela Superior Politécnica del Chimborazo, Riobamba, Ecuador.

***Abstract*—This work presents an improvement of transient stability of the Galapagos hybrid system using and UPFC device, besides it assess the conditions that allow this system to keep stability at steady-state conditions and regain a stable operating point after being subjected to a severe disturbance. Is performed given the changes in the configuration of the system due to growth and, also, for future expansions ´ planned, and is based on the analysis of the results obtained with the computational Power Factory tool**

Index terms*— *Introduction, power flow control unit, smallsignal, Transient stability.

I. INTRODUCTION

The Unified Power Flow Controller (UPFC) is one of the facts more versatile than can be used for the control and optimization of power flow; this can operate as STATCOM and SSSC to improve the reliability indices of the system and the power flow.

This research work has as objective to analyze the conditions of transient stability of Galapagos hybrid system without the incorporation of the UPFC and with the UPFC, for this will simulate contingencies with the Software Power Factory 15.1.7 to examine the response of the system with and without the UPFC applying some contingencies.

II. DESCRIPTION OF THE STUDY CASE

A. Photovoltaic and Energy Storage System in Baltra.

The Project is located on the Baltra Island that implements a hybrid system with a 67 kWp photovoltaic power plant, 4300 kWh energy storage system and 1,000 kW of fossil power plants.

B. Baltra Wind Park

Wind Park of 2.25 MW formed by three wind turbines located on the island of Baltra and that are connected with the electrical system of the Santa Cruz Island through the Electric Interconnection System Baltra – Santa Cruz of 34.5 kV.

C. Photovoltaic Plant Puerto Ayora.

Photovoltaic plant of 1500 kWp of installed capacity, located in the town of Puerto Ayora, Santa Cruz Island. Include 6006 photovoltaic panels and connects to the substation Puerto Ayora through an overhead line to 13.8 kV.

D. Thermoelectric Plant Santa Cruz

Thermoelectric plant located in the town of Puerto Ayora that comprises of 9 diesel generators.

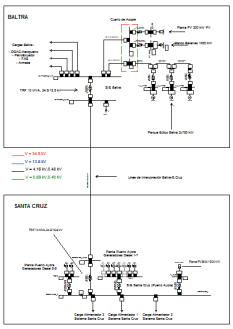

Fig. 1. Hybrid System Galapagos

III. UNIFIED POWER FLOW CONTROLLER - UPFC

A. Description of the UPFC

Unified driver of power flows (UPFC) consists of two converters in voltage source (VSC) one connected in parallel and other connected in series. If switches 1 and 2 are open, the two converters act as STATCON and SSC controlling the current and voltage injected in series and parallel respectively in the line. When you close the switchs 1 and 2 the two converters are in capacity to exchange active power among themselves. [3]

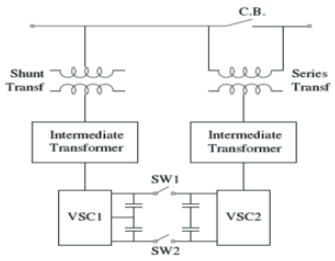

Fig. 2. Diagram of the UPFC

B. Model of the UPFC in Steady State

The converter in parallel consumes power for each one of its branches Ir and Ip.

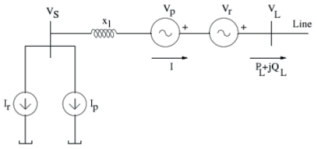

Fig. 3. Model of stable state of UPFC

The apparent power SL is given by:

$$SL = PL + jQL = I^{*}VL = \frac{VL^{*} - VR^{*}}{-jXL} * VL = \frac{VL^{2} - VR^{*}VL}{-jXL} \quad (1)$$

Where:

$$VR = V\angle - \frac{\delta}{2} \quad (2)$$

$$VL = Vs + Vc = V\angle\frac{\delta}{2} + Vc\angle\beta \quad (3)$$

Active PL and reactive QL power can be expressed such as:

$$PL = Po + \frac{VVc}{XL} sin\left(\frac{\delta}{2} + \beta\right) \quad (4)$$

$$QL = Qo + \frac{Vc^{2}}{XL} - \frac{VVc}{XL} cos\left(\frac{\delta}{2} + \beta\right) + \frac{2VVc}{XL} cos\left(\frac{\delta}{2} - \beta\right) \quad (5)$$

Qo' expression is:

$$Q'_{0} = Qo + \frac{Vc^{2}}{XL} \quad (6)$$

Finally working on β, from (1) and (2) we have:

$$(PL - Po)^{2}(5 - 4\cos\delta) + (QL - Qo')^{2} - 4(PL - Po)(QL - Qo')\sin\delta = \frac{V^{2}Vc^{2}}{XL}(2\cos\delta - 1)^{2} \quad (7)$$

C. Dynamic model UPFC

Figure 4 shows a diagram of a UPFC, where XSH AND XSR are the parallel and serial ballasts of the transformer respectively.

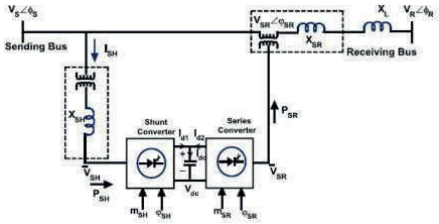

Fig. 4. Transmission line with UPFC

DC currents Id1 and Id2 showed at fig. 4. , voltage and currents of the capacitor have the following harmonic relationships:

$$I_{dc} = C\,\frac{dV_{dc}}{dt} \quad (8)$$

$$I_{dc} = I_{d1} + I_{d2} \quad (9)$$

For the AC system, it is known that P_{SH} and P_{SR} can be calculated as follows:

$$P_{SH} = R_{e}(V_{SH}I_{SH}^{*}) = R_{e}(V_{SH}(\frac{V_{S} - V_{SH}}{jX_{SH}})^{*}) \quad (10)$$

$$P_{SR} = R_{e}(V_{SR}I_{L}^{*}) = R_{e}(V_{SR}(\frac{V_{S} + V_{SR} - V_{R}}{j(X_{SH} + X_{L})})^{*}) \quad (11)$$

Applying the PWM control, for the two converters of sources of voltages, relations of investors DC - AC can be expressed as follows:

$$V_{SH} = \frac{m_{SH}V_{dc}}{2\sqrt{2}V_{B}} \quad (12)$$

$$V_{SR} = \frac{m_{RH}V_{dc}}{2\sqrt{2}V_{B}} \quad (13)$$

Finally taking the relationship of the transformer in series as 1:1 can be obtain the equations of the UPFC used for the dynamic model, so:

$$CV_{dc}\frac{dV_{dc}}{dt} = (P_{SH} - P_{SR})S_{B} \quad (14)$$

Where:

$$P_{SH} = R_{e}(V_{SH}(\frac{V_{S} - V_{SH}}{jX_{SH}})^{*}), P_{SR} = R_{e}(V_{SR}(\frac{V_{S} + V_{SR} - V_{R}}{j(X_{SR} + X_{L})})^{*}) \quad (15)$$

$$V_{SH} = (m_{SH}V_{dc}/V_{B})\lfloor(\emptyset_{S} - \varphi_{SH}) \quad (16)$$

$$V_{SR} = (m_{SR}V_{dc}/V_{B})\lfloor(\emptyset_{S} - \varphi_{SH}) \quad (17)$$

A good reference about UPFC behavior is [7]

IV. PHOTOVOLTAIC POWER STATION

A. Theoretical Model of Solar Panel

The solar panel is the result of associate a set of photovoltaic cells in series.

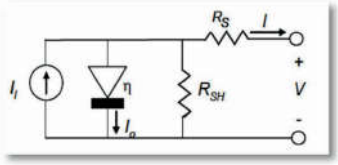

Fig. 5. Basic electric model of photovoltaic cell

$$I = I_{I} - I_{0}\left(e^{\frac{V + R_{S}I}{\eta V_{t}}} - 1\right) - \frac{V + R_{S}I}{R_{SH}} \quad (18)$$

$$I_{I} = Area * \left(J_{SC}\frac{G}{1000} + \alpha_{J_{SC}}(T - 27)\right) \quad (19)$$

Where the area: $[m^{3}]$, J_{SC} is the density of short-circuit current$\left[A/_{cm^{2}}\right]$, T: working temperature [°C], $\alpha_{J_{SC}}$: Temperature [°C], Factor $\left[A/_{°C.cm^{2}}\right]$, G: Irradiance $\left[W/_{cm^{2}}\right]$

$$I_{0} = \frac{J_{SC}.Area.T_{K}^{3}.e^{-\frac{Eg}{V_{t}}}}{\left(e^{\frac{Voc}{\eta V't}} - 1\right).300^{3} - \frac{E'g}{V'_{t}}} \quad (20)$$

Where I0: saturation current, Vt: thermal voltage [V], Eg: Energy of GAP [eV], VOC: open circuit voltage [V], TK: Temperature in Kelvins

$$V_{t} = \frac{K.T_{k}}{q} \quad (21)$$

Where K: Boltzmann Constant q: charge of an electron

$$E_g = E_{g0} - \frac{\alpha_{gap} T_k^2}{\beta_{gap} + T_k} \quad (22)$$

B. Association of Elements

The model offers the possibility of concentrating a bank of solar panels in a single panel or models each of them separately, having to associate a higher level circuit later.
Then the following equations can be applied in the calculation of the voltage and current
o

$$V_g = \sum_{i=1}^{N_{sg}} V_{ci} \approx N_{sg}.V_c \quad (23)$$

$$I_g = \sum_{i=1}^{N_{pg}} I_{ci} \approx N_{pg}.I_c \quad (24)$$

This simplification is also valid for determining the parameters characteristic of the panel.

$$V_{oc_g} = \sum_{i=1}^{N_{sg}} V_{oc_i} \approx N_{sg}.V_{oc} \quad (25)$$

$$I_{sc_g} = \sum_{i=1}^{N_{pg}} I_{sc_i} \approx N_{pg}.I_{sc} \quad (26)$$

The following equation raises the assumption of maximum power disipable by a solar cell and the formula of the expression of the security zone.

$$I_g.\sum_{i=1}^{N_s-1} V_i < P_{máx} \quad (27)$$

$$V_g > (N_{sg}-1)\left(V_{oc} + V_i \ln\left(1 - \frac{I_g}{N_{pg}.I_{sc}}\right)\right) - \frac{P_{max}}{I_g} N_{pg} \quad (28)$$

II. BATTERY

A. Modeling Battery

In figure 6 shows a battery based on the model of Copetti

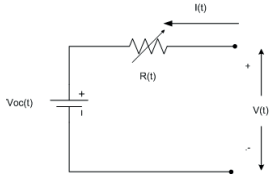

Fig. 6. Copetti Models

$$R_{in}(t) = f1(I(t), \Delta T(t), SoC(t)) \quad (29)$$

$$V_{oc}(t) = f2(SoC(t)) \quad (30)$$

$$SoC(t) = \frac{1}{C(t)}\left(SoC + \int_0^t \eta(\omega) \cdot I(\omega) \cdot d\omega\right) \quad (31)$$

Where *I(t)* is the current flowing in the battery. ΔT(t) is the difference of temperature of the electrolyte with respect to 25°C and SoC(t) is the state of charge of the battery on the other hand, the instant ability C(t) is:

$$C(t) = \frac{C_{nom} \cdot C_c}{1 + A_c\left(\frac{|I(t)|}{I_{nom}}\right)^{B_c}} \cdot \left(1 + q1_c \cdot \Delta T(t) + q2_c \cdot \Delta T^2(t)\right) \quad (32)$$

Where Cnom is the nominal capacity of the battery obtained a discharge current Inom, and Ac, Bc, Cc, q1c and q2c are tuning parameters.

B. Battery operation zones

- *Download zone:* It happens when *I (t) <0.*

$$V(t) = \left(V_{0d} - K_{od} \cdot (1 - SoC(t))\right) \quad (33)$$

$$-\frac{|I(t)|}{C_{10}} \cdot \left(\frac{P_{1d}}{1 + |I(t)|^{P_{2d}}} + \frac{P_{3d}}{SoC(t)^{P_{4d}}} + P_{5d}\right) \cdot (1 - q_d \cdot \Delta T) \quad (34)$$

- *Load Zone:* It happens when I (t)> 0.

$$V(t) = \left(V_{0c} - K_{oc} \cdot (SoC(t))\right) \quad (35)$$

$$+\frac{|I(t)|}{C_{10}} \cdot \left(\frac{P_{1c}}{1 + |I(t)|^{P_{2c}}} + \frac{P_{3c}}{(1 - SoC(t))^{P_{4c}}} + P_{5c}\right) \cdot (1 - q_c \cdot \Delta T) \quad (36)$$

- *Overload zone:* In this zone of operation is distinguished I (t)> 0 and V> Vg

$$V(t) = V_g(t) + \left(V_m(t) - V_g(t)\right) \cdot \left(1 - e^{\frac{\left(LoE(t) \cdot C_n - SoC_g(t) \cdot C(t)\right)}{I(t) \cdot \tau(t)}}\right) \quad (37)$$

$$V_g(t) = \left(A_g + B_g \cdot ln(1 + \frac{I(t)}{C_{10}})\right)\left(1 - q_g \Delta T\right) \quad (38)$$

$$V_m(t) = \left(A_m + B_m\left(1 + \frac{I(t)}{C_{10}}\right)\right)(1 - q_m \Delta T) \quad (39)$$

$$\tau(t) = \frac{A_t}{1 + B_\tau\left(\frac{I(t)}{C_{10}}\right)^{C_\tau}} \quad (40)$$

- *Transition zone:* To avoid numerical problems looking for a continuous transition between the loadings and unloading zone.

$$V(t) = \left(\frac{V_c|I_d - V_d|I_d}{2 \cdot I_d}\right) \cdot I(t) + \frac{V_c|I_d + V_d|I_d}{2} \quad (41)$$

V. MODEL OF WIND TURBINE POWERED DOBLEMENTE

A. General.

This wind turbine model is in direct connection to the mains, operates at variable speed due to its static frequency converter AC / DC / bidirectional AC, which supplies voltage and variable rotor windings of the induction generator frequency type.

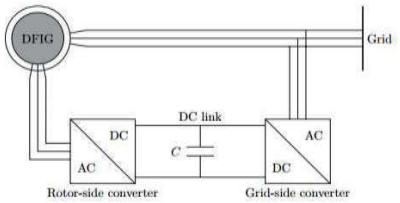

Fig. 7. DFIG model

B. The DFIG model

For the development of the model of the DFIG assumes the following premises: the voltage in DC is considered constant at all times. In addition to despise the stator resistance within the model, the converter function on the side of the network is to ensure the correct operation of the side of the rotor by a factor of unity and only active power is transmitted to the network.

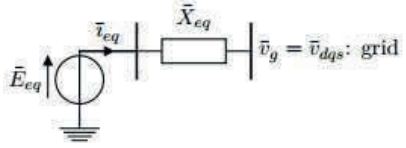

Fig. 8. DFIG Equivalent circuit

C. Analysis in the steady state

The equivalent circuit that can be used in a stable state for the double fed generator is presented below, which is detailed in the form single phase, but is due to a three-phase composition.

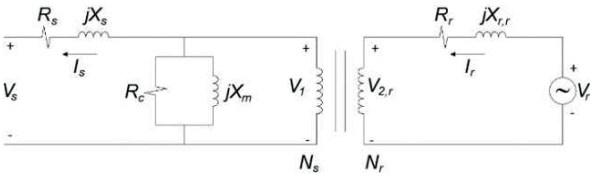

Fig. 9. Steady state equivalent circuit

The detailed previously circuit that dynamically represents the DFIG can be expressed in terms of the variables relating to the rotor stator, using the relationship of turns of the winding as shown below.

$$\frac{R_r'}{s} = a^2 \cdot \frac{R_r}{s} \quad (42)$$

$$X_r' = a^2 \cdot X_r \quad (43)$$

$$\frac{V_r'}{s} = a \cdot \frac{V_r}{s} \quad (44)$$

There is a circuit, considering the inclusion of the active power flows in the double fed induction generator to disregard the losses in the nucleus, as shown below.

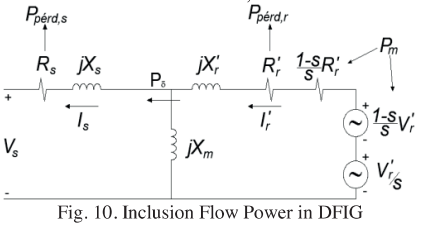

Fig. 10. Inclusion Flow Power in DFIG

The mechanical power Pm is expressed as:

$$P_m = 3 \cdot \frac{1-s}{s} \cdot R_r' \cdot |I_r'|^2 - 3 \cdot \Re\left\{\frac{1-s}{s} \cdot V_r' \cdot I_r'^*\right\} \quad (45)$$

While the power transmitted from the rotor to the stator through the air gap P_δ is:

$$P_\delta = P_m - P_{pérd,r} \quad (46)$$

$$P_\delta = P_m - 3 \cdot R_r' \cdot |I_r'|^2 \quad (47)$$

Finally, the resulting power in the stator without considering the core losses is:

$$P_s = P_\delta - P_{pérd,s} \quad (48)$$

$$P_s = P_\delta - 3 \cdot R_s \cdot |I_s|^2 \quad (49)$$

According to the operation of the DFIG can be a state generator synchronous sub where the rotor speed is lower than the synchronous speed, so the slip is positive and a super state where the synchronous speed of the rotor is greater than the speed synchronous, so the slip is negative.

D. Dynamic Analysis Machine's Simulation:

For the dynamic modeling must raise the equations of links of flows.

$$\frac{d}{dt}\psi_{qs} = \omega_b \cdot \left[v_{qs} - \frac{\omega}{\omega_b} \cdot \psi_{ds} + \frac{r_s}{X_{ls}} \cdot (\psi_{mq} - \psi_{qs})\right] \quad (50)$$

$$\frac{d}{dt}\psi_{ds} = \omega_b \cdot \left[v_{ds} + \frac{\omega}{\omega_b} \cdot \psi_{qs} + \frac{r_s}{X_{ls}} \cdot (\psi_{md} - \psi_{ds})\right] \quad (51)$$

$$\frac{d}{dt}\psi_{0s} = \omega_b \cdot \left[v_{0s} - \frac{r_s}{X_{ls}} \cdot \psi_{0s}\right] \quad (52)$$

$$\frac{d}{dt}\psi_{qr}' = \omega_b \cdot \left[v_{qr}' - \left(\frac{\omega - \omega_r}{\omega_b}\right) \cdot \psi_{dr}' + \frac{r_r'}{X_{lr}'} \cdot (\psi_{mq} - \psi_{qr}')\right] \quad (53)$$

$$\frac{d}{dt}\psi_{dr}' = \omega_b \cdot \left[v_{dr}' + \left(\frac{\omega - \omega_r}{\omega_b}\right) \cdot \psi_{qr}' + \frac{r_r'}{X_{lr}'} \cdot (\psi_{md} - \psi_{dr}')\right] \quad (54)$$

$$\frac{d}{dt}\psi_{0r}' = \omega_b \cdot \left[v_{0r}' - \frac{r_r'}{X_{lr}'} \cdot \psi_{0r}'\right] \quad (55)$$

$$X_{aq} = X_{ad} = \left(\frac{1}{X_M} + \frac{1}{X_{ls}} + \frac{1}{X_{lr}'}\right)^{-1} \quad (56)$$

In function of the equations of links of flow can be find the equations of current in the dynamic model of the DFIG as shown below.

$$i_{qs} = \frac{1}{X_{ls}} \cdot (\psi_{qs} - \psi_{mq}) \quad (57)$$

$$i_{ds} = \frac{1}{X_{ls}} \cdot (\psi_{ds} - \psi_{md}) \quad (58)$$

$$i_{0s} = \frac{1}{X_{ls}} \cdot \psi_{0s} \quad (59)$$

$$i_{qr}' = \frac{1}{X_{lr}'} \cdot (\psi_{qr}' - \psi_{mq}) \quad (60)$$

$$i_{dr}' = \frac{1}{X_{lr}'} \cdot (\psi_{dr}' - \psi_{md}) \quad (61)$$

$$i_{0r}' = \frac{1}{X_{lr}'} \cdot \psi_{0r}' \quad (62)$$

The electromagnetic torque expression in current terms and flow links per second is:

$$T_e = \psi_{ds} \cdot i_{qs} - \psi_{qs} \cdot i_{ds} \quad (63)$$

Finally, the rotor angular speed is solved by:

$$\frac{d}{dt}\omega_r = \frac{\omega_b}{2 \cdot H} \cdot (T_e - T_L) \quad (64)$$

DFIG model can be expressed through the following block diagram.

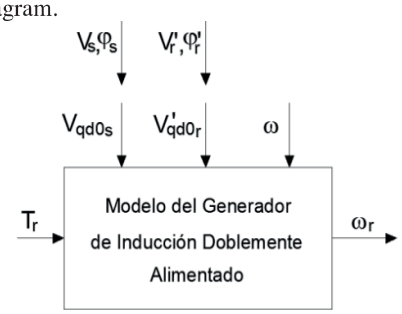

Fig. 11. DFIG equivalent model

VI. APPLICATION TO PROJECT

In this system to place the UPFC in the line that connects the two substations, opened a section of the line in the node V16 which is closest to the half of the line as shown below in Fig.11 [3]

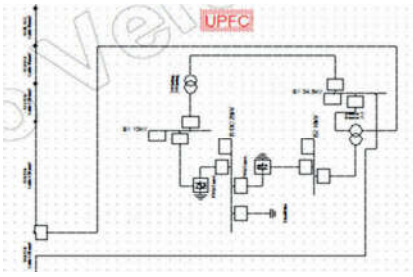

Fig. 12. UPFC model

The UPFC was modeled using the "Power Factory" and the other necessary parameters are obtained from system simulation, they are the following:

Table I.
THREE-PHASE TWO-WINDING TRANSFORMER´S DATA
(mayúsculas)

Three-phase two-winding transformer	
Primary Voltage	34.5 kV
Primary Voltage	10 kV
Power	0.6 MVA

Table II.
THREE-PHASE TRANSFORMER BOOSTER'S DATA
(mayusculas)

Three-phase transformer Booster	
Primary Voltage	10 kV
Primary Voltage	10 kV
Power	1.9 MVA

VII. CONTINGENCIES RESULTS

A. *Unseasonable generator output WTG_1 located in Baltra, without UPFC.*

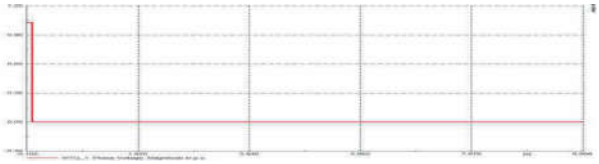

Fig. 13. Voltage generator

- *Active and reactive power in the generator*

The following figures show the contribution of the active and reactive power, these are zero because the WTG_1 generator is out of service.

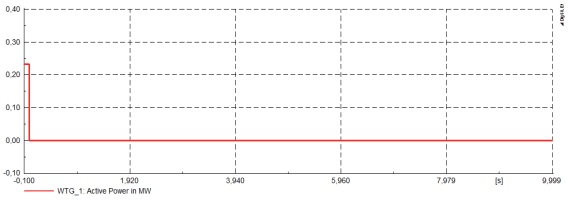

Fig. 14. Active power generator

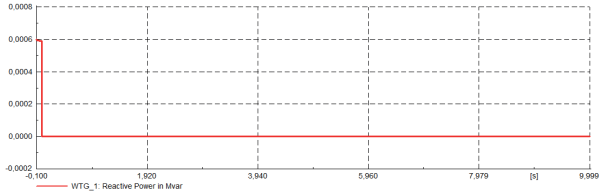

Fig. 15. Reactive power generator

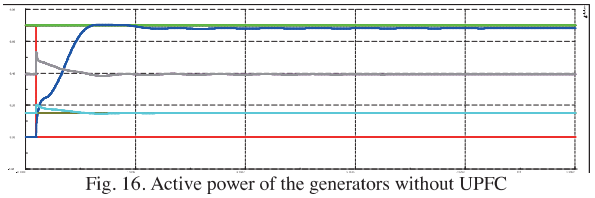

Fig. 16. Active power of the generators without UPFC

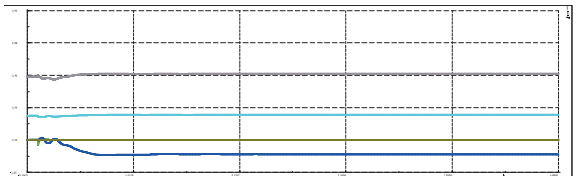

Fig. 17. Reactive power of the generators without UPFC

- *Voltages at the buses of Baltra*

The following figures shows that the voltages of the bars of Baltra, range during the disconnection of the generator, but is reset.

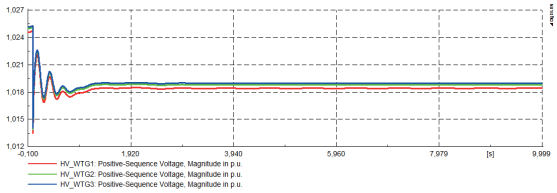

Fig. 18. Voltajes en las barras de Baltra

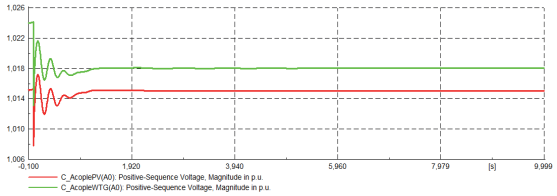

Fig. 19. Voltajes en las barras de Baltra

When you connect the UPFC in the system and creates an event of erratic output of the generator WTG_1. By default the UPFC tends to protect the rest of the system off the generation points or banks of batteries, isolating the failure.

B. *Unseasonable generator output WTG_1 located in Baltra, with UPFC.*

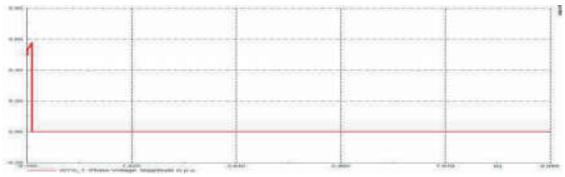

Fig. 20. Voltage generator

- *Active and reactive power in the generator*

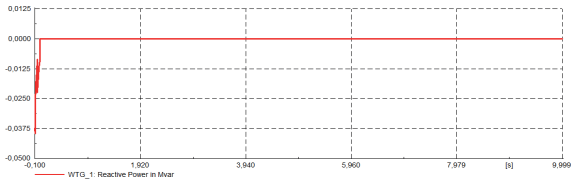

Fig. 21. Active and Reactive power in WTG 1

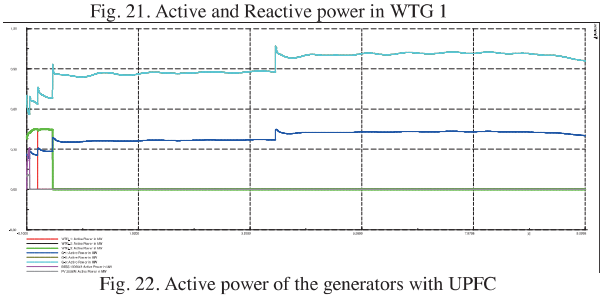

Fig. 22. Active power of the generators with UPFC

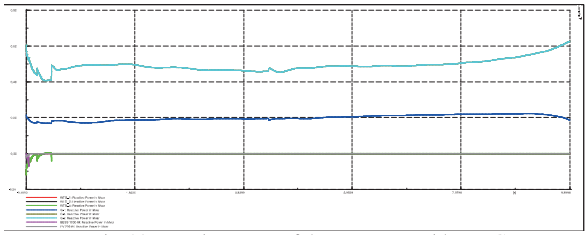

Fig. 23. Reactive power of the generators with UPFC

- *Voltages at the buses of Baltra*

As a disconnection from all sources, usually the system collapses without oscillations, however the application of UPFC's in power system prevents damage to system components.

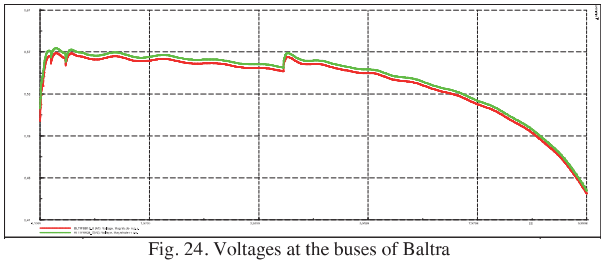

Fig. 24. Voltages at the buses of Baltra

C. Short circuit simulations BLTR/BB34_5(V0) bus Three phase short circuit, without UPFC

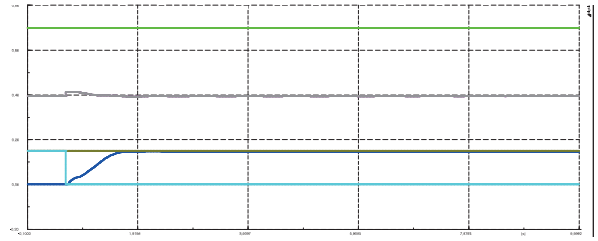

Fig. 25. Active power from Generators without UPFC

D. Short circuit simulations BLTR/BB34_5(V0) bus Three phase short circuit, with UPFC

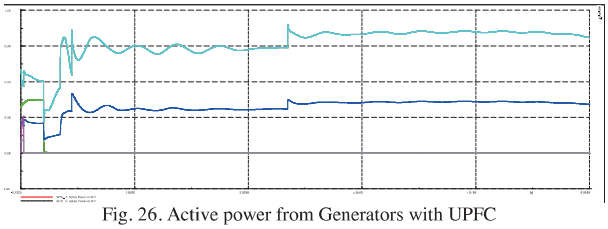

Fig. 26. Active power from Generators with UPFC

VII. CONCLUSIONS

Although the literature presents a number of works which consider the UPFC for voltage and power control, there are few texts that presented in detail the inclusion process in POWER FACTORY software.

The UPFC should be considered as a separate branch from the network, it must have the equations to govern its dynamic and the corresponding DSL implementation, so inclusion in the SEP for a power flow does not change directly the results in bars systems.

VIII. REFERENCES

[1] Narain G. Hingorani, Laszlo Gyugyi. Understanding FACTS, IEEE Press, 2000.

[2] Pinnarelli, De Martinis, Andreotti, "Modelling of unified Power Flow Controller into Power System using PSpice.", IPST 2001- paper 205, Ago 2001.

[3] Fujita, Watanabe, Akagi, "Control and analysis of a Unified Power Flow Controller." IEEE Transaction on Power electronics, Vol. 14, no. 6, pp. 1021-1027, Nov-99.

[4] Cerda, S. y Palma, R. (2004). Modeling and incorporation of the unified driver of power flow in the optimal power flow. Thesis, Engineering Department be electrical, University of Chile, 2004.

[5] Hingorani, N. and Gyugyi, L. (2000). Understanding FACTS: concepts and technology of flexible AC transmission systems. IEEE Power Engineering Society, IEEE Press; ISBN 0780334558

[6] Kyriakides, E. and Suryanarayanan, S. (2006). Surveys-based assessment of i nternational power engineering education programs. Power Engineering Society General Meeting, 2006. IEEE 18-22 June 2006.

[7] Masuda, M.; Bormio, E.; Jardini, J. A.; Silva, F. A. T.; Copeliovitch, S. and Camargo, J. (2004). Development and implementation of FACTS devices in distribution networks. IEEE/PES Transmisión and Distribution Conference and Exposition: Latin America. 2004, pp. 839- trabajos científicos", 2005, Roberto Day

VIII. BIOGRAPHIES

Carlos Fabián Gallardo. - received the B.S and M.Sc degrees from Flensburg University, Flensburg, Germany, in 1999 and 2005, respectively, and the Ph.D degree from Carlos III University of Madrid, Madrid, Spain, in 2009, all in Electrical Engineering.

He is currently an Associate Professor at Energy Department in Escuela Politécnica Nacional University, Quito, Ecuador.

His research interests include Power Systems Analysis and Control, FACTs. HVDC and PETs Modelling and Control

Mayra Espinoza.- received the B.S and M.Sc degrees from Escuela Superior Politécnica de Chimborazo University, Riobamba, Ecuador in 1994, and 2000, respectively, and the Ph.D degree from Escuela Superior Politécnica de Chimborazo, Riobamba,